Accepted Manuscript

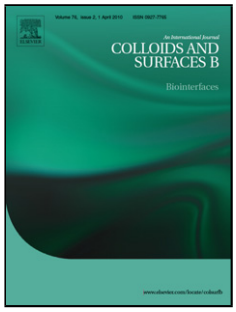

Title: A sensitive biosensing method for detecting of ultra-trace amounts of AFB1 based on "Aptamer/reduced graphene oxide" nano-bio interaction

Authors: Amirkhosro Beheshti-Marnani, Abdolhamid Hatefi-Mehrjardi, Zarrin Es'haghi

PII: S0927-7765(18)30878-6
DOI: https://doi.org/10.1016/j.colsurfb.2018.11.087
Reference: COLSUB 9852

To appear in: *Colloids and Surfaces B: Biointerfaces*

Received date: 9 August 2018
Revised date: 19 November 2018
Accepted date: 30 November 2018

Please cite this article as: Beheshti-Marnani A, Hatefi-Mehrjardi A, Es'haghi Z, A sensitive biosensing method for detecting of ultra-trace amounts of AFB1 based on "Aptamer/reduced graphene oxide" nano-bio interaction, *Colloids and Surfaces B: Biointerfaces* (2018), https://doi.org/10.1016/j.colsurfb.2018.11.087

A sensitive biosensing method for detecting of ultra-trace amounts of AFB1 based on "Aptamer/reduced graphene oxide" nano-bio interaction

Amirkhosro Beheshti–Marnani[a*], Abdolhamid Hatefi-Mehrjardi[a], Zarrin Es'haghi[a]

[a]Department of Chemistry, Payame Noor University (PNU), P.O.Box:19395-4697,Tehran, Iran.

Amirkhosro_b@yahoo.com

Hatefi: hhatefy@yahoo.com

Eshaghi : zarrin_eshaghi@yahoo.com

Graphical abstract

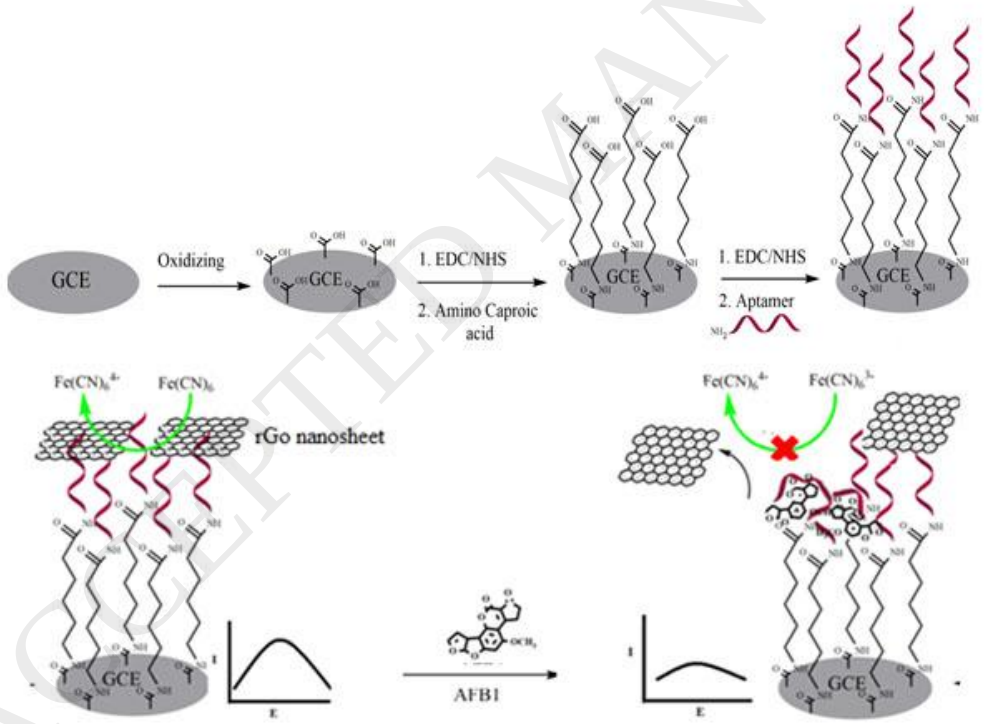

a

Highlights

1) An aptasensor, was fabricated for detecting ultra-low levels of aflatoxin B1.
2) Behavior of modified electrodes was studied in presence of reduced graphene.
3) Differential pulse voltammetry was applied for determination of aflatoxin B1.

Abstract

A simple, low-cost and sensitive label-free aptasensor assembled with assisting reduced graphene oxide nanosheets as the signal amplifier was fabricated and applied for detecting ultra-low levels of Aflatoxin B1(AFB1) through a nano-bio interaction system. The conditions of different modified glassy carbon electrodes as the base of aptasensor were investigated by cyclic voltammetry (CV), differential pulse voltammetry (DPV) and electrochemical impedance spectroscopy (EIS). The performance of the fabricated aptasensor was evaluated by FESEM, HRTEM and AFM images. The proposed biosensor detected AFB1sensitively in a wide linear range (0.5nM-4µM) by DPV with a considerable low limit of detection (LOD=0.07nM) and good repeatability (RSD=2.9) and stability. Finally, the present aptasensor was applied successfully for monitoring AFB1 with appropriate recoveries in pasteurized cow milk and human blood plasma as real samples.

Keywords: Aptasensor, Label-free, Biosensor, Aflatoxin B1, Nano-bio interaction.

1. Introduction

Aflatoxins are a subcategory of mycotoxins, which are produced by *Aspergillus* fungi and are known as mutagen and carcinogen even at very low quantities [1].The permitted concentration of Aflatoxin B1(AFB1) available in food categories is reported by European Union [2]. Moreover, Aflatoxin B1is the most poisonous type of its family and can convert to type M_1 in liver and kidneys [3]. In this regard, ultra-trace determination of AFB1 can undoubtedly be very important. Few novel methods in the recent literature which are applied for the sensitive determination of Aflatoxin B1 with low detection limits are photoluminescence-based immunosensing[4],high-performance liquid chromatography[5],indirect competitive ELISA[6] along with "absorption spectrometry"[7]. Extensive investigation about nucleic acids led to the synthesis of a specific type with a strong ability to bind to target molecules like proteins, drugs and other biomolecules. These nucleic acids are called "aptamer" [8] .Indeed, the aptamers are the synthetic antibodies from DNA or RNA assisted with ligands or functional groups (with no effect on the aptamer properties).In general, aptamers were prepared by SELEX(selection evolution of ligands by exponential enrichment) method[9].Certainly, aptamers are more

stable than antibodies and have ability to be applied in different settings [10].An important property of aptamers that makes them suitable for "aptasensing", is their reversible denaturation and resistance against changing properties ,which may originate from binded ligands and functional groups. Electrochemical aptasensors have some advantages over other biosensing methods (such as immunosensors) due to their ability of re-naturation after de-naturation for several times, which makes them more economical along with high stability [11-13]. Moreover, biosensors based on aptamers are simpler compared to complicated, less sensitive and time-consuming methods such as spectrometry and HPLC [14-16].

Commonly, labeled electrochemical aptasensors are consisted of covalent and noncovalent labels. The label species can grant more analytical sensitivity via providing a large surface area for electroactivity and stabilize the aptamer immobilization [17]. Despite the mentioned advantages, the labels bound to aptamers may affect aptamer properties like the disturbance in double helix formation of aptamer with its target as well as time consuming. Also, selecting of labeling positions may be a challenge due to the need to minimize the interference between the label and folding process of the aptamer. On the other hand, small electrochemical labels may not be appropriate because of the small perturbance after interaction with aptamers [18]. This is while label-free aptamers are exempted from these problems [19].

A number of investigations have been performed through the label – free aptasensing like: prostate specific antigen detecting using various platforms and nanomaterials such as mesoporous silica thin film[20], metal oxide microstructures [21], carbon nanotubes[22] and other nano-scale materials[23].

"Graphene" as a two-dimensional carbonaceous nanomaterial, has significant conductivity [24]. Additionally, the graphene nanosheets with edge defects can be appropriate mediators for fast electron transferring and analytical signal promoter in electrochemical aptasensing[25].Graphene nanosheets can physiochemically interact with biological molecules like membranes, DNA, aptamers along with the changes in kinetic and electro-catalytic effects. Such interactions are called "nano-bio interface" [26,27].

In the current work, a label-free aptasensor was fabricated based on immobilization of a single strand DNA (ssDNA) aptamer on the surface of glassy carbon electrode (GCE), as a simple platform, for detecting Aflatoxin B1 in ultra-low levels of concentrations with a wide linear range. Reduced graphene oxide (rGO) nanosheets could bind to aptamer from the other side of the assembled sandwich through π-π interactions that significantly decreased the charge transfer resistance related to red/ox process of the electrochemical probe($K_4[Fe(CN)_6]$/ $K_3[Fe(CN)_6]$.Herein, the considerable event was the ability of noncovalent adsorption related to π-π interactions between graphene hexagonal nanosheets and pyrimidine/puric bases of the unfolded aptamer,

which formed a nano-bio interface interaction. Obviously, the folded strands of aptamer abandoned the reduced graphene nanosheets. In this way, the specified adsorption of the AflatoxinB1 (target) could proportionally influence the binding of graphene nanosheets to the aptamer. Cyclic voltammetry (CV) and electrochemical impedance spectroscopy (EIS) characterized the modified glassy carbon electrodes. Differential pulse voltammetry (DPV) was applied for performing the quantitative analysis of Aflatoxin B1 in real samples with significant results.

2. Experimental

2.1. Chemicals and instrumentals

$K_4[Fe(CN)_6]$ and $K_3[Fe(CN)_6]$, as the electrochemical probes, EDC (1-Ethyl-3-(3-dimethylaminopropyl) carbodiimide), NHS(*N*-Hydroxysuccinimide) and 6-aminohexanoic acid (Aminocaproic acid), as coupling reagents and Aflatoxin B1(AFB1) in 1:1 V/V methanol: chloroform were purchased from Sigma-Aldrich. Phosphate buffer (PBS) was prepared by using calculated quantities of NaCl, $MgCl_2$, Na_2HPO_4, KH_2PO_4, and Cl^-. All of the chemical reagents used during the aptasensor assembling were from Merck in analytical grades. Human blood plasma belonged to healthy persons was prepared from the “Iranian blood transfusion organization”.

AFB1 binding ssDNA aptamer was synthesized through SELEX method and functionalized with the C_6-NH_2 group with the following sequence (purchased from Bioneer, Republic of Korea):

5′ NH_2-C_6- GTTGGGCACGTCTTGTCTCTCTGTGTCTCGTGCCCTTCGCTACGCCCACA-3′

OD=5, Length=50bases, MW=15433.07

A 100μM stock solution of aptamer was prepared by diluting with sterilized and deionized water and kept frozen for following experiments.

FESEM and HRTEM images were obtained by MIRALL TESCAN and Philips CM30, 300 kV respectively. X-ray diffraction data were collected using a Phillips PW 1800 diffractometer with Cu Kα radiation.

Also, electrochemical experiments such as CV and DPV were performed by potentiostat/galvanostat model Origaflex500 (Orygalys, France).Impedance tests (EISs)were performed in an open circuit potential equal to 0.23V versus Ag/AgCl with frequency from 10KHz till 0.01Hz by Autolab potentiostat/galvanostat supported by FRA software,(from The Netherlands).All the tests were done in three-electrode system including standard glassy carbon electrode (1mm in diameter) as the working electrode, Ag/AgCl electrode as the reference and a platinum auxiliary electrode .

2.2. Synthesis of reduced graphene nanosheets (rGO)

Graphene oxide (Go) were prepared by modified Hummers' method [28]. In order to convert graphene oxide to the reduced form (rGO), the graphene oxide suspension in deionized water was ultrasonicated for 30 min. Then it was transferred to a dialyzed bag for 24h in order to separate the agglomerated particles. A mixture of 5ml of 25%amonia solution and 5 ml of hydrazine hydrate 50% w/w were added to 0.3 mg/ml of graphene oxide suspension. The solution stirred during reflux in 95º C for 1h. The obtained solution consisted of reduced graphene nanosheets (rGO) was ultrasonicated for 20 min before each use. FESEM and HRTEM images were prepared from synthetic rGO.

2.3. Fabrication of the AFB1aptasensor

In order to activate the surface of glassy carbon electrode (1mm in diameter) with -CO, -OH , -COOH and epoxy groups, the polished bare GCE was inserted in 0.5M of H_2SO_4 and seven cycles applied on the bare GCE in range of 0.9-1.5V with scan rate equal to 80mV/S through cyclic voltammetry method. Then the electrode was washed with deionized water and immersed in a 5ml of EDC and NHS (5 and 7 mg respectively as coupling mediators) mixture dissolved in PBS(0.1M, pH=5.5) at room temperature for 1h.

After that, the electrode was rinsed carefully with the same buffer and deionized water and then immediately inserted in 5ml of PBS (0.1M, pH=7.5) including

0.025g of aminocaproic acid and 0.1M of KCl for 1h in room temperature. Amino- caproic acid(6-aminohexanoic acid) plays the role as the spacer that creates an opportunity for aptamer conformation and mobility as well as greater strength for aptamer adsorption on the surface of electrode. Then the washed electrode was inserted again in 5ml of a fresh mixture of EDC and NHS (5 and 7 mg respectively) dissolved in PBS (0.1M, pH=5.5) for 1h. Finally, the electrode was rinsed carefully with deionized water and 10µl of AFB1binding ssDNA aptamer with optimized concentration (as described later) dropped on the surface of the electrode in room temperature.

The steps of electrode modification are shown schematically in fig.1.

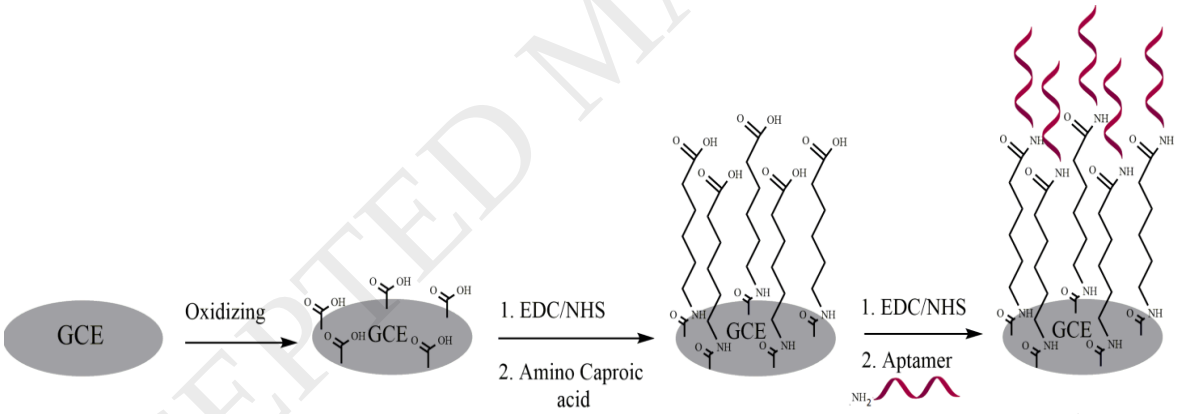

Fig.1, Schematic diagram of glassy carbon electrode modification steps leading to ssDNA aptamer immobilization.

Also, in order to understand the interaction among the ssDNA AFB1aptamer and reduced graphene nanosheets, AFM images of three different cases of electrodes (bare glassy carbon electrode (GCE), the GCE which was modified,

as described above, inserted in 10nM and 10µM of AFB1 respectively and then incubated with 0.3 mg/ml of rGO) were obtained.

3. Results and discussion

3.1. Characterization of modified GCEs

Fig.2A and 2B show the successful synthesis of reduced graphene nanosheets by FESEM and HRTEM images respectively. As can be seen, the morphology and transparency of graphene sheets are being observed obviously. Fig.2a, 2b and 2c are related to AFM images of bare GCE and Aptamer immobilized GCEs that firstly reacted with 10nM and 10µM of AFB1 respectively and then incubated with 0.3 mg/ml of rGO to forming GCE/modified/aptamer/AFB1(10nM)/rGO and GCE/modified /aptamer/AFB1(10µM)/rGO. As can be seen, rGO nanosheets have left their binded positions on modified electrodes because of increase in the concentration of AFB1(from10nM to 10 µM) as the result of forming more aptamer-target double helixes.Fig.2C schematically shows the events occurred after increasing the concentration of AFB1which is in agreement with AFM images.

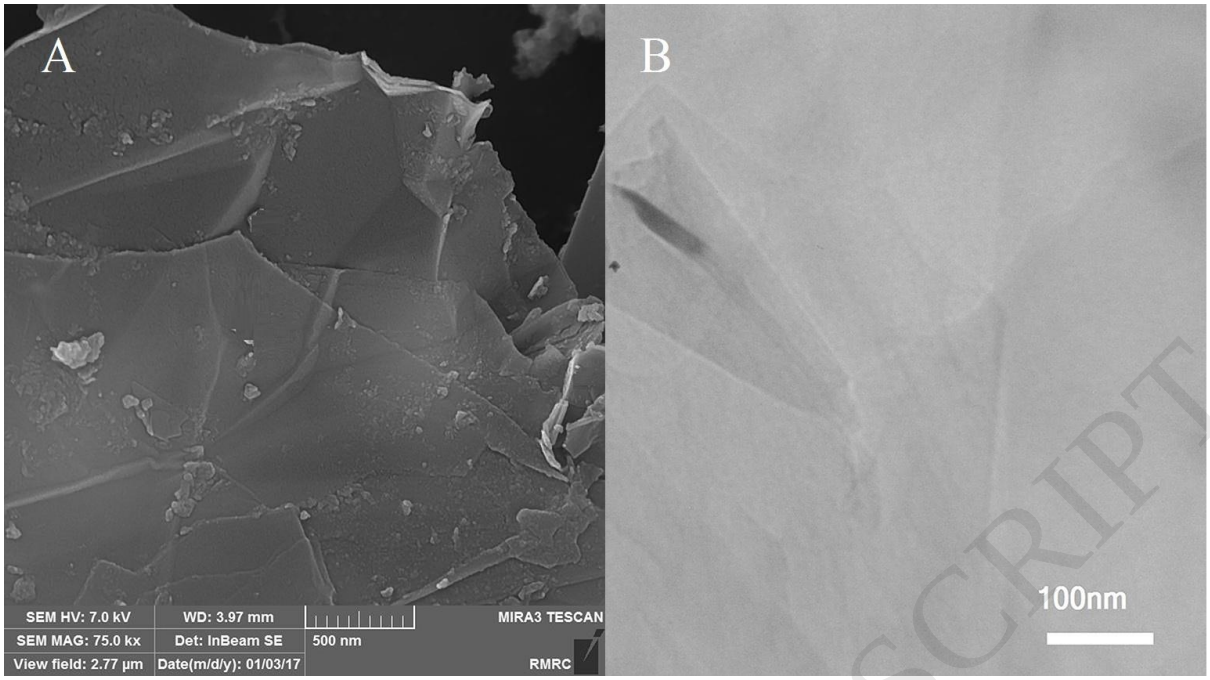

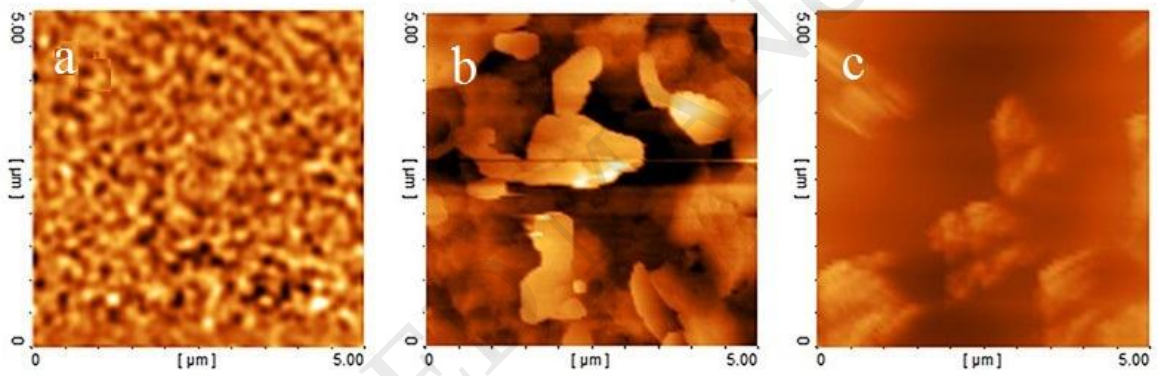

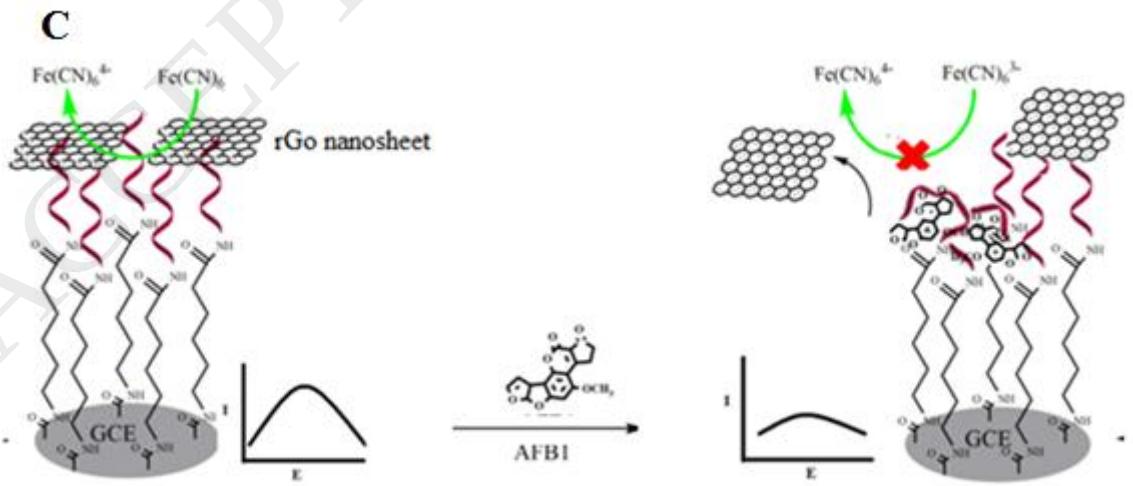

Fig. 2: (A) FESEM image of synthetic reduced graphene nanosheets (rGO), (B) HRTEM image of rGO that shows transparent sheets,and AFM images of (a)bare glassy carbon electrode (GCE),(b) GCE/modified/aptamer/AFB1(10nM)/rGO and (c) GCE/modified /aptamer/AFB1(10µM)/rGO.(C) Schematic diagram that illustrates: with entrancing moreAFB1 molecules to forming the double helix , the signal drops simultaneously with leaving rGO nanosheets from their binding positions.

3.2. Electrochemical studies

3.2.1. Optimization of aptamer concentration and investigation of the electrochemical behavior of modified electrodes

For assuring the best results through quantitative analysis with maximum responses, optimization of the amounts of aptamer immobilized on the surface of the electrode is necessary. For this propose. various concentrations of aptamer (10,25,50,75,85 and 100µM) for immobilizing step were used with a high constant concentration ofAFB1 (10µM). As can be observed from the cyclic voltammograms in fig. 3, the current response from 50 µM of the aptamer to upper values remained almost constant. Consequently, the 50 µM of the aptamer was selected as the optimum concentration of aptamer with assuming maximum double helix formation capacity in following experiments. The corresponding DPVs also confirmed the CVs responses (inset of fig.3).

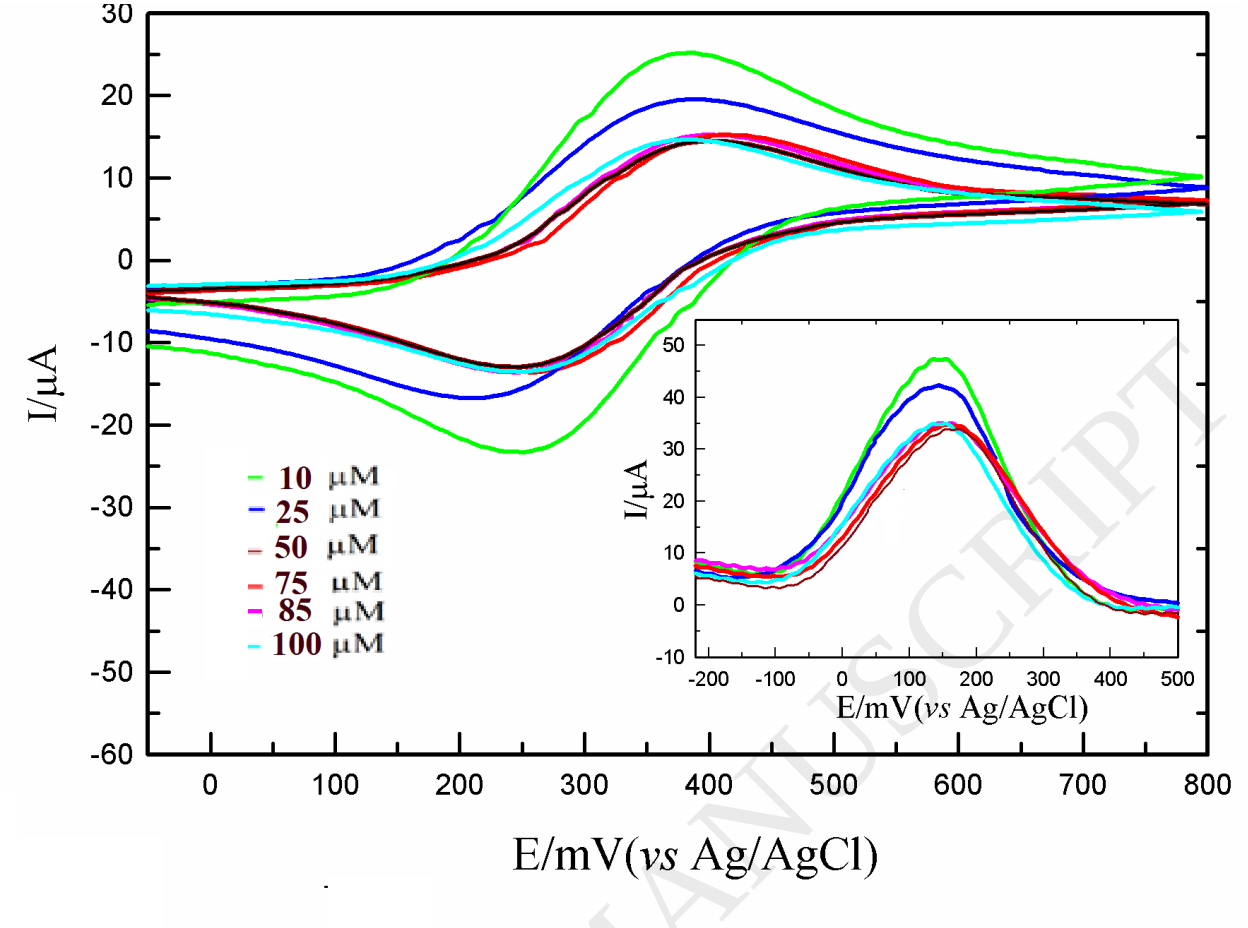

Fig.3.Cyclic voltammograms of modified GCEs with different concentrations of aptamer (10, 25,50, 75,85 and 100 µM) reacted with 10 µM of AFB1 with scan rate equal to 30mV/S in presence of 0.007M of $K_3[Fe(CN)_6]$ /$K_4[Fe(CN)_6]$ in PBS (0.1M, pH=7) as the probe. Inset: Corresponding DPVs that confirms the same trend.

To survey the behavior of modified electrodes as well the effect of reduced graphene nanosheets on electron transfer, cyclic voltammograms were obtained for various modified electrodes in presence of 0.007M of $K_3[Fe(CN)_6]$ /$K_4[Fe(CN)_6]$ in PBS (0.1M, pH=7) as the electrochemical probe.

As can be seen in fig 4.A,the highest anodic peak current (46µA)has belonged to the modified electrode which was applied with the optimized amount of aptamer(obtained in the previous section) and incubated with 0.3 mg of rGO for 1h(GCE/modified/aptamer/rGO).The lowest anodic peak current belonged to the modified electrode which firstly reacted with 1µM of AFB1 for 1h and then incubated with 0.3 mg of rGO (GCE/modified/aptamer/AFB1/rGO).It suggests that double helix formation of aptamer with its target could be as an effective obstacle against diffusing the probe to the surface of the electrode. The voltammograms between these two cases were related to different modified GCEs that showed meaningful electrochemical behavior. The role of reduced graphene nanosheets, which binded to aptamer via π-π interactions in facilitating electron transfer, was clearly seen in these series of cyclic voltamogramms. The impressive comparison was between GCE/modified/aptamer/AFB1/rGO and GCE/modified/aptamer/AFB1.As can be seen in fig.4A (d) and (e), the difference between peak currents shows the significant effect of reduced graphene nanosheets in facilitating charge transfer despite of hindrance originated from double helixes formed by the aptamer-target system. It is suggested that rGO nanosheets get the opportunity to bind with unreacted aptamers via π-π interactions in case GCE/modified/aptamer/AFB1/rGO.

For further confirmation and certainty of the electrochemical behavior of different modified electrodes, electrochemical impedance spectroscopy (EIS) as Nyquist plots were obtained in presence of 0.007M of $K_3[Fe(CN)_6]$ /$K_4[Fe(CN)_6]$ under the same conditions which were described before. The plots and the circuit model for the fitting of the related data are shown in fig4. B.

As expected, the lowest charge transfer resistance (R_{ct}) evidently was belonged to GCE/modified /aptamer/rGO. Predictably, the large resistance against charge transfer was seen for GCE/modified/aptamer/AFB1due to steric inhibition caused by the formation duplexes of aptamer with its target. Also, the negative charge of the immobilized aptamer (due to negative phosphate backbone) in case GCE/modified/aptamer, was repelled the probe ($[Fe\ (CN)_6]^{3-/4-}$) which is negatively charged. So, a large R_{ct} was obtained relative to GCE/modified with no immobilized aptamer. Obviously, existence of the rGO binded to the aptamer, effectively reduced the charge transfer resistance compared to GCE/modified/aptamer/AFB1 (fig.4B (d) and (e). In case GCE/modified /aptamer/rGO, a lot of amounts of rGO nanosheets could binded noncovalently to nucleobases of the aptamer and significant decrease in R_{ct} value was observed(fig.4B(a)). On the other hand, a small decrease in R_{ct} was observed for GCE/modified/aptamer/AFB1/rGO(fig.4B (d)).This is because; formation a stable double helix between aptamer and AFB1partially consumed the

accessible positions for reacting with rGO nanosheets. Also, this fact was previously observed through comparison of AFM images (fig.2b and c).

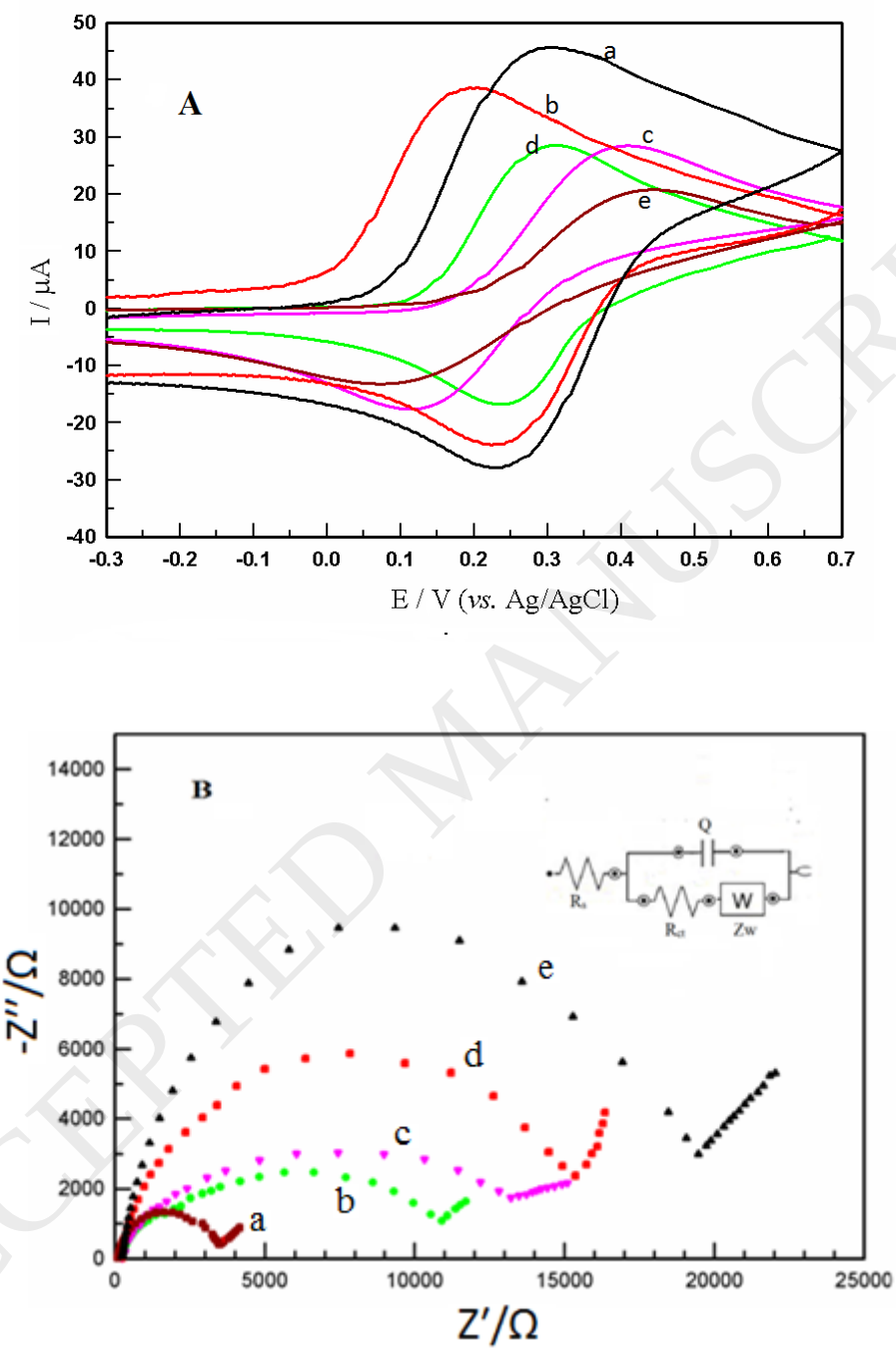

Fig.4:(A) Cyclic voltammograms and (B) EIS responses of various modified GCEs:(a) GCE/modified/aptamer/rGO,(b)GCE/modified,(c)GCE/modified/aptamer,(d):GCE/modified/ aptamer /AFB1/rGO and (e): GCE/modified/aptamer /AFB1.(inset of fig 4.B:circuit model of

EIS: R_s,R_{ct} ,Q and Z_w stand for the solution resistance, resistance against charge transfer from solution to surface of electrode, constant phase element and Warburg impedance related to contribution diffusion respectively).

3.2.2. DPV detection of Aflatoxin B1 by developed label- free aptasensor

Herein, GCE/modified/aptamer was prepared with the optimum immobilized aptamer, and firstly reacted with various concentrations (0.5 nM to 4µM) of the target, AFB1, for 1h and then incubated with rGO nanosheets (0.3 mg/ml) during 1hour for every concentration. As described schematically in fig.2C, with increasing the AFB1concentration, more duplexes were formed and the DPV response of the probe was decreased (fig.5A).

A calibration plot (fig.5B) was obtained by using the difference between peak current of blank and the other concentrations (ΔI), versus logarithmic values of concentrations (Log C). A linear plot was obtained in the wide range of 0.5 nM to 4 µM of AFB1.The significant low value of LOD was obtained equal to 0.07nM by using $3S_b/b$, which S_b stands for the standard deviation of seven responses of blank solution and b represents the slope of the calibration curve. Repeatability of the prepared aptasensor was calculated 2.9% as a remarkable relative standard deviation (RSD%) regard to five times detections of 50 nM of AFB1 and corresponded currents. The stability of the developed aptasensor was tested by keeping it in PBS (0.1M, pH=7.5) at 4ºC during a week. Dropping in

current responses less than 4%, was seen for determination the same concentration of AFB1 (50nM), that confirmed the satisfying stability of the proposed aptasensor.

Overall, the modified electrode as the aptasensor showed a good linear response (0.998) with a wide range, good sensitivity, significant detection of limit (LOD), appropriate RSD and stability with the perfect and simple methodology for quantitative proposes.

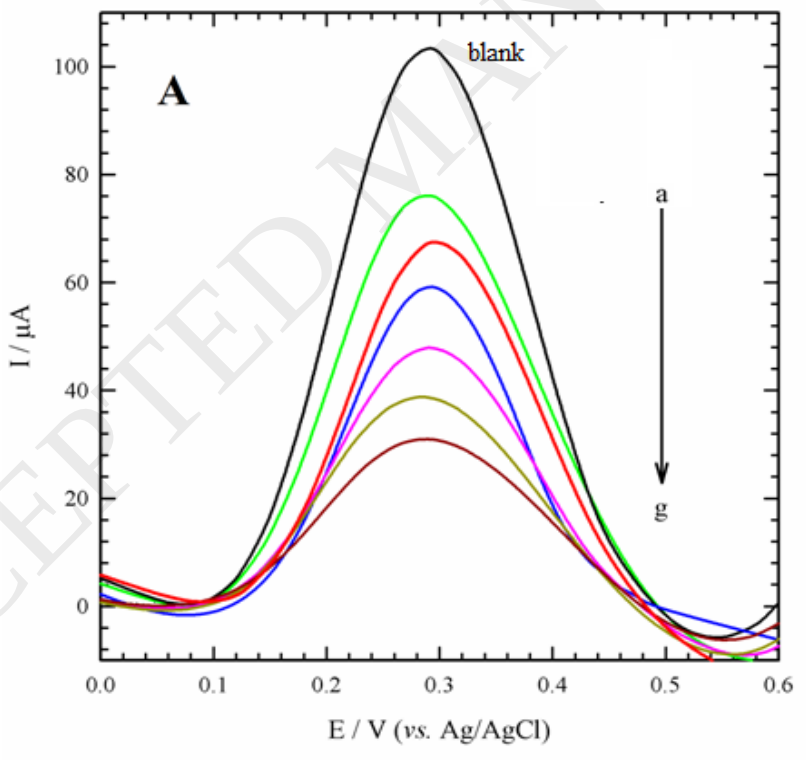

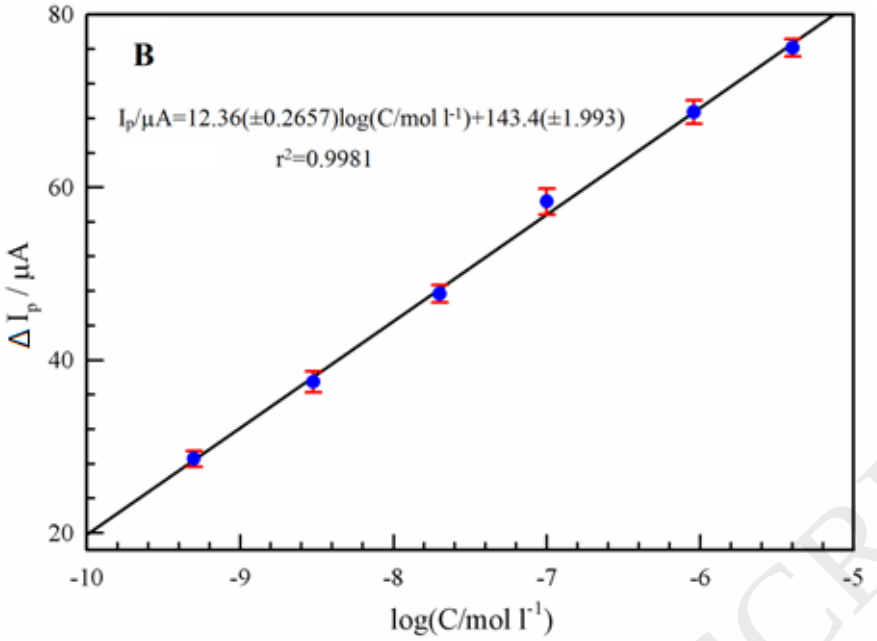

Fig.5, (A): DPV responses of probe for different concentrations of AFB1,(a) 0.5nM, (b) 3nM,(c)20nM,(d)100nM,(e)0.9µM and(f) 4µM for "GCE/modified/aptamer that firstly reacted with various concentrations of AFB1 before incubating with 0.3mg/ml rGO for 1h"(scan rate=80mV/S, step=6mV, pulse=50mV and pulse time=5msec)(B):The calibration plot resulted from corresponded currents.

Table .1 shows the comparison among a few reports of bionsensing that mostly used as aptasensors for AFB1 determination. The obtained results by the current study confirmed a wide Linear range, significant LOD, and sensitivity except for the aptasensor that was based on polycarboxylic macrocycle which showed the lower detection of limit [30]. However, our wider concentration range and better RSD could compensate for this disadvantage.

Table .1. Comparison of proposed aptasensor characteristics with recent works.

Modified electrode	**Linear range of AFB1concentration**	**LOD**	**RSD%**	**Ref.**
Quantum dots-aptamer-GO fluorescence quenching	3.2nM-320µM	1nM	Not reported	[29]
Aptasensor based on Polycarboxylic macrocycle	0.1nM-100nM	0.05nM	3.50	[30]
Aptamer-based biosensor using PAMAM dendrimers	0.1nM-10nM	0.25nM	Not reported	[31]
Aptamer-based Colorimetric	80nM-270nM	7nM	Not reported	[32]
Aptamer conjugated quantum dots adsorbed on AuNPs	10nM-400nM	3.4nM	Not reported	[33]
Acetylcholinesterase-based conductometric biosensor	0.25mM - 1 mM	0.16µM	7.00	[34]
Current work	0.5 nM- 4 µM	0.07nM	2.9	--------

The developed label-free aptasensor was applied for real sample analysis. Few analytical samples of human blood plasma and pasteurized cow milk were prepared. The specified amounts of AFB1 spiked in real samples without any pretreatments. Four concentrations were selected in the linear range (500, 50, 0.5 and 0.0nM of AFB1). Considerable recovery percentages were obtained in the range of 94.58-104% by standard addition method that are shown with details in table.2. The results acquired in this section showed successful usage of our simple label- free aptasensor for real sample analysis.

Table .2. Obtained results of real sample analysis

Sample	AFB1 spiked (nM)	AFB1 detected (nM)	Recovery (%)	RSD (%)
Human blood plasma	500	492.15	98.43	2.94
	50	488.20	97.64	3.04
	0.5	0.52	104.00	3.43
	0.0	Not detected	----	----
Pasteurized cow milk	500	472.90	94.58	3.11
	50	47.93	95.68	3.27
	0.5	0.51	102.82	3.68
	0.0	Not detected	----	----

4. Conclusion

In this work, the surface of the bare glassy carbon electrode (GCE) was firstly oxidized and then the AflatoxinB1(AFB1) ssDNA aptamer was immobilized on the surface of GCE via coupling reagents. Through this manner, a simple label-free aptasensor was designed and developed with assisting reduced graphene nanosheets as a signal amplifier through nano-bio interaction. Differential pulse voltammetry (DPV) was applied for the determination of AFB1in real samples. The very low detection limit was calculated 0.07nM beside of a wide range linearity (R^2=0.998) and good sensitivity. Successful application of the low -

cost apt sensor for real sample analysis with good recovery percentages promisingly led to monitoring the Aflatoxin B1 in food and biological samples.

REFERENCES

[1] M. F. L. Lemos, C. A. M. Van Gestel, A. M. V. M. Soares, Developmental toxicity of endocrine disrupters bisphenol A and vinclozolin in a terrestrial isopod, Arch. Environ. Contam. Toxicol. 59(2) (2010) 274-281.

[2] H. J. Ok, H. E. Kim, W. B. Shim, H. Lee, D. H. Bae, D. H. Chung, H. S. Chun, Natural occurrence of aflatoxin B1 in marketed foods and risk estimates of dietary exposure in Koreans, J. Food Prot. 70(12) (2007) 2824-2828.

[3] E. E. Creppy, Update of survey, regulation and toxic effects of mycotoxins in Europe, Toxicol. Lett. 127(1-3) (2002) 19-28.

[4] V. Myndrul, R.Viter, M. Savchuk, M. Koval. N. Starodub, V. Silamiķelis,V. Smyntyna, A. Ramanavicius, I. Iatsunskyi, Gold coated porous silicon nanocomposite as a substrate for photoluminescence-based immunosensor suitable for the determination of Aflatoxin B1, Talanta. 175 (2017) 297-304.

[5] P.D. Andrade, J. L. da Silva, E. D. Caldas, Simultaneous analysis of aflatoxins B1, B2, G1, G2, M1 and ochratoxin A in breast milk by high-performance liquid chromatography/fluorescence after liquid–liquid extraction with low temperature purification (LLE–LTP), J. Chromatogr. A. 1304 (2013) 61-8.

[6] D. Kong, Z. Xie, L. Liu, S. Song, H. Kuang, G. Cui, C. Xu, Development of indirect competitive ELISA and lateral-flow immunochromatographic assay strip for the detection of sterigmatocystin in cereal products, Food Agric Immuno. 28(2) (2017) 260-273.

[7] D. Bueno, G. Istamboulie, R. Muñoz, J. L. Marty, Determination of mycotoxins in food: a review of bioanalytical to analytical methods, Appl. Spectrosc. Rev. 50(9) (2015) 728-774.

[8] M. Shahdordizadeh, S. M. Taghdisi, N. Ansari, F. A. Langroodi, K. Abnous, M. Ramezani, Aptamer based biosensors for detection of Staphylococcus aureus, Sens. Actuators B-Chem. 241(2017) 619-35.

[9] K.H. Lee, H. Zeng, A general double library SELEX strategy for aptamer selection using unmodified nonimmobilized targets, Anal. Bioanal. Chem. 409(21) (2017) 5081-5089.

[10]A. Sassolas, L. J. Blum, D, B. D. Leca-Bouvier, Electrochemical aptasensors, Electroanalysis. 21(11) (2009) 1237-1250.

[11] A. Rahi, N. Sattarahmady, H. Heli, Label-free electrochemical aptasensing of the human prostate-specific antigen using gold nanospears. Talanta. 156 (2016) 218-224.

[12]Y. Zheng, Y.Yuan,Y. Chai, R.Yuan, A label-free electrochemical aptasensor based on the catalysis of manganese porphyrins for detection of thrombin, Biosen. Bioelectron. 66 (2015) 585-589.

[13] K. Wang, J. Liao, X. Yang, M. Zhao, M. Chen, W. Yao, W. Tan, X. Lan, A label-free aptasensor for highly sensitive detection of ATP and thrombin based on metal-enhanced PicoGreen fluorescence, Biosens. Bioelectron. 63 (2015) 172-177.

[14] J.A. Osorio-Guarín, J. Berdugo-Cely, R. A. Coronado, Y. P. Zapata, C. Quintero, G. Gallego-Sánchez, R. Yockteng, Colombia a source of cacao genetic diversity as revealed by the population structure analysis of germplasm bank of theobroma cacao L, Front. Plant Sci. 8 (2017), p.1994.

[15] G. Liang, Y. Man, A. Li, X. Jin, X. Liu, L. Pan, DNAzyme-based biosensor for detection of lead ion: a review, Microchem. J. 131 (2017) 145-53.

[16] A. Gutiérrez, E. N. Primo, M. Eguílaz, C. Parrado, M. D. Rubianes, G. A Rivas, Quantification of neurotransmitters and metabolically related compounds at glassy carbon electrodes modified with bamboo-like carbon nanotubes dispersed in double stranded DNA, Microchem. J.130 (2017) 40-46.

[17] L.Yang, X. Zhang, M. Ye, J. Jiang, R.Yang, T. Fu, Y. Chen, K. Wang, C. Liu, W.Tan, Aptamer-conjugated nanomaterials and their applications. Adv. Drug Deliv. Rev, 63(14-15) (2011) 1361-1370.

[18] T. Hianik, J. Wang, Electrochemical aptasensors–recent achievements and perspectives, Electroanalysis. 21(11) (2009) 1223-1235.

[19] W. Mok, Y. Li, Recent progress in nucleic acid aptamer-based biosensors and bioassays, Sensors, 8(11) (2008) 7050-7084.

[20] W. Argoubi, A. Sánchez, C. Parrado, N. Raouafi, R. Villalonga, Label-free electrochemical aptasensing platform based on mesoporous silica thin film for the detection of prostate specific antigen. Sens. Actuators B- Chem. 255(2018) 309-315.

[21] Y. L. Deng, D.D. Xu, D. W. Pang, H.W .Tang ,Target-triggered signal turn-on detection of prostate specific antigen based on metal-enhanced fluorescence of Ag@ SiO2@ SiO2-RuBpy composite nanoparticles, Nanotechnology. 28(6) (2017). p. 065501.

[22] F. Tahmasebi, A. Noorbakhsh, Sensitive electrochemical prostate specific antigen aptasensor: effect of carboxylic acid functionalized carbon nanotube and glutaraldehyde linker. Electroanalysis. 28(5) (2016) 1134-1145.

[23] J. Shi, J. Lyu, F. Tian, M. Yang, A fluorescence turn-on biosensor based on graphene quantum dots (GQDs) and molybdenum disulfide (MoS2) nanosheets for epithelial cell adhesion molecule (EpCAM) detection, Biosens. Bioelectron. 93 (2017) 182-188.

[24] R. Raccichini , A. Varzi , S. Passerini , B. Scrosati , The role of graphene for electrochemical energy storage, Nat. Mater. 14(3) (2015), p. 271

[25] J. Ping, Y. Zhou, Y. Wu Papper, S. Boujday, R. S. Marks, T. W. Steele. Recent advances in aptasensors based on graphene and graphene-like nanomaterials, Biosens. Bioelectron. 64 (2015) 373-385.

[26] Y Wang, Z. Li, J. Wang, J. Li, Y. Lin. Graphene and graphene oxide: biofunctionalization and applications in biotechnology, Trends Biotechnol. 29(50) (2011) 205-212

[27] A. E. Nel, L. Mädler, D. Velegol, T. Xia, E.M.Hoek, P. Somasundaran, F. Klaessig, V. Castranova, M .Thompson, Understanding biophysicochemical interactions at the nano–bio interface. Nat Mater, 8(7) (2009), p. 543.

[28] W. Mok, Y.Li. Recent progress in nucleic acid aptamer-based biosensors and bioassays, Sensors. 8(11) (2008) 7050-7084.

[29] Z. Lu, X. Chen, Y. Wang, X. Zheng, C.M. Li, Aptamer based fluorescence recovery assay for aflatoxin B1 using a quencher system composed of quantum dots and graphene oxide. Microchim Acta. 182(3-4) (2015) 571-578.

[30] G. Evtugyn, A. Porfireva, V. Stepanova, R. Sitdikov, I. Stoikov, D. Nikolelis, T. Hianik, Electrochemical aptasensor based on polycarboxylic macrocycle modified with neutral red for aflatoxin B1 detection, Electroanalysis. 26(10) (2014) 2100-2109.

[31] G. Castillo, K. Spinella, A. Poturnayová, M. Šnejdárková, L. Mosiello, T. Hianik, Detection of aflatoxin B1 by aptamer-based biosensor using PAMAM dendrimers as immobilization platform. Food Control. 52 (2015) 9-18.

[32] M. Hosseini, H. Khabbaz, M. Dadmehr, M. R.Ganjali, J. Mohamadnejad, Aptamer-based colorimetric and chemiluminescence detection of aflatoxin B1 in foods samples, Acta Chim. Slov. 62(3) (2015) 721-728.

[33] F.S. Sabet, M. Hosseini, H. Khabbaz, M. Dadmehr, M.R. Ganjali, FRET-based aptamer biosensor for selective and sensitive detection of aflatoxin B1 in peanut and rice. Food Chem. 220 (2017) 527-532.

[34] O.O. Soldatkin, O. S Burdak,T. A. Sergeyeva, V. M. Arkhypova, S.V. Dzyadevych, A. P Soldatkin, Acetylcholinesterase-based conductometric biosensor for determination of aflatoxin B1. Sens. Actuator B-Chem. 188 (2013) 999-1003.